

Synthesis of epoxide and vicinal diol regioisomers from docosahexaenoate methyl esters

Mike VanRollins,¹ Peter D. Frade, and Oscar A. Carretero

Hypertension Research and Clinical Chemistry Divisions, Henry Ford Hospital, Detroit, MI 48202

Abstract Docosahexaenoic acid (22:6(n-3)) was recently shown to be metabolized by liver microsomes to vicinal diol regioisomers. To identify the diols, and to compare their biological actions with those of epoxide precursors, we developed a chemical method to synthesize microgram to milligram amounts of epoxides and corresponding diols. In brief, methylated docosahexaenoate was reacted for 15 min with 0.1 eq *m*-chloroperoxybenzoic acid. After normal- and reverse-phase high performance liquid chromatography, six products were isolated. The underivatized or hydrogenated products were characterized and identified using capillary gas-liquid chromatography and mass spectrometry. The products were identified as 19,20-, 16,17-, 13,14-, 10,11-, 7,8-, and 4,5-epoxydocosapentaenoate. Per incubation, the total epoxide yield from 22:6(n-3) was 8.6%. By reincubating unused substrate 10-20 times (cycling), the total epoxide could be increased to 55-70%. As found for epoxides of arachidonic and eicosapentaenoic acids, the yield of individual regioisomers increased as the distance between the targeted double bond and carbomethoxy group increased. Each epoxide regioisomer was hydrolyzed to its corresponding vicinal diol. The gas-liquid chromatographic retention times and mass spectra of the diol products were found to match those of metabolites produced by cytochrome P-450 monooxygenases.—VanRollins, M., P. D. Frade, and O. A. Carretero. Synthesis of epoxide and vicinal diol regioisomers from docosahexaenoate methyl esters. *J. Lipid Res.* 1989. 30: 275-286.

Supplementary key words n-3 fatty acids • docosahexaenoic acid • epoxides • cytochrome P-450

The cytochrome P-450 system oxidizes arachidonic acid 20:4(n-6) along three major pathways: ω -hydroxylation, ω 2-hydroxylation, and epoxygenation. In turn, the epoxygenase metabolites are hydrolyzed to vicinal diols by microsomal or cytosolic hydrolases. Cytochrome P-450 monooxygenases also oxidize 20:4(n-6) along a minor pathway to lipoxigenase-like metabolites. Thus, there exist four distinct pathways by which cytochrome P-450 monooxygenases oxidize 20:4 (n-6).

Most of the cytochrome P-450 metabolites of 20:4(n-6) have been unequivocally identified by matching their mass spectra and chromatographic properties with those of synthesized standards. In addition, homologous ω -hydroxy, ω 2-hydroxy, diol, and lipoxigenase-like metabolites from docosahexaenoic acid (22:6(n-3)) and eicosapentaenoic acid (20:5(n-3)) have been characterized chromatographically and by mass spectrometry (1, 2). However, the epoxide metabolites of 22:6(n-3) and 20:5(n-3) have yet to be characterized (1, 2). The first objective of the present study was to synthesize standards to aid in identifying the epoxides and the corresponding diols formed from 22:6(n-3). The second objective was to synthesize these standards in microgram to milligram amounts so that the biological actions of epoxides and diols from 22:6(n-3) could be compared to those found for 20:4(n-6) (reviewed in ref. 3). We now report on a simple method for the synthesis of microgram to milligram quantities of epoxides and diols from 22:6(n-3).

MATERIALS

Technical grade *m*-chloroperoxybenzoic acid (*m*-CIPBA) was purchased from Aldrich Chemical Co. (Milwaukee,

Abbreviations: n:d(n-a), "n" and "d" represent the number of carbons and double bonds, respectively; the locant (upper) of the terminal double bond is (n-a) carbons from the carboxyl of the fatty acid, and "a" represents the number of carbon atoms between the nth carbon and the terminal bond. *m*-CIPBA, *m*-chloroperoxybenzoic acid; ODS, octadecasilyl; TLC, thin-layer chromatography; RP- and NP-HPLC, reverse-phase and normal-phase high performance liquid chromatography; GLC-MS, gas-liquid chromatography-mass spectrometry; ECL, equivalent chain length.

¹To whom correspondence and reprint requests should be addressed at: Hypertension Research Division, Henry Ford Hospital, 2799 West Grand Boulevard, Detroit, MI 48202.

WI). This reagent (lot 47F3403 was 80.7% pure; *m*-chlorobenzoic acid was the major impurity) was stored at 4°C in a desiccator and was used within 1–3 months from its purity determination. Methyl 22:6(n-3), more than 99% pure, was purchased from Nu-Chek-Prep, (Elysian, MN). Tracer [1-¹⁴C]22:6(n-3), obtained from New England Nuclear (Boston, MA), had a specific radioactivity of 55 Ci/mol. This tracer was only 97% radiopure, as judged by RP-HPLC and TLC.

Organic solvents of high performance liquid chromatography (HPLC) grade (Omnisolve) were purchased from EM Science (Cherry Hill, NJ). Just before use, house-deionized water was cycled through a Nanopure II (with Organic Free cartridge) and Organipure system (Barnstead, Boston, MA). All organic solvents and water were vacuum-filtered (0.22 μm GVW, Millipore Corp., Bedford, MA) before being mixed. In addition, solutions were prepared in large volumes (2,000 ml) so as to nearly fill the HPLC reservoirs (Omnifit, Cambridge, England). The pre-mixed solutions were then sonicated under vacuum for 1 min, and returned to ambient pressure with helium (99.995% pure, Air Products, Chicago, IL). After being sparged with helium for 5 min, each solution was maintained under a helium blanket. Solutions prepared in this manner virtually eliminated the water-soluble contaminants seen at 192 nm during gradient steps, reduced alterations in retention times due to evaporation effects, and minimized drift in absorption at 192 nm due to O₂ influx.

Analytical and semi-preparative HPLC were performed with a pump system which consisted of a 50 or 200 μl loop injector (#7125, Rheodyne, Cotati, CA), a column temperature controller with solvent-heating module (CH-1448, Systec, Inc., Minneapolis, MN), two dual-reciprocating-piston pumps (M6000A, Waters Assoc., Milford, MA), a dynamic dual mixer (Beckman, San Ramon, CA), a gradient controller (#720, Waters), and two in tandem variable-wavelength detectors (SF783G, Kratos Analytical Instruments, Ramsey, N.J.; LC-95, Perkin Elmer, Norwalk, CT).

METHODS

Preparation of methylated substrate

Tracer [1-¹⁴C]22:6(n-3) was diluted with unlabeled 22:6(n-3) to a specific radioactivity of 70 nCi/mg. After being methylated with ethereal diazomethane, the substrate was isolated by reverse phase (RP-) HPLC. In brief, the methylated 22:6(n-3) was dissolved in 200 μl methanol, and injected onto a semi-preparative column (1 (i.d.) × 25 cm, 5-μm ODS particles, Ultrasphere, Beckman, Irvine, CA). Development was done at 4 ml/min with CH₃CN-H₂O 70:30 (v/v). Methylated 22:6(n-3) was visualized by

monitoring absorption at 192 nm, and was collected at 39 min. Upon removal of CH₃CN by vacuum, methylated 22:6(n-3) was extracted into five vol of CH₂Cl₂, concentrated under a nitrogen stream, and stored in methanol at -80°C. Methylated 22:6(n-3) was > 99% pure chemically and radiochemically, based on RP-HPLC in which radioactivity and absorption at 192 and 237 nm were monitored.

Generation of epoxides

Epoxidation of 22:6(n-3) was done using *m*-CIPBA which converts *cis* double bonds into (+/-) *cis*-epoxides (4). In brief, 10 mg of radiolabeled methyl 22:6(n-3) was dissolved in 0.5 ml CH₂Cl₂, and added to a vacuum hydrolysis tube (Pierce Chemical Co., Rockford, IL) containing a magnetic stirring bar. Then 0.1 eq *m*-CIPBA, dissolved in 0.5 ml CH₂Cl₂, was added dropwise over 1.5 min. Immediately thereafter, the hydrolysis tube was capped and its contents were stirred at 30°C for 15 min. To remove the by-product *m*-chlorobenzoic acid, the reaction mixture was mixed (Big Vortexer, Glas-Col, Terre Haute, IN) for 2 min with 1 ml ice-cold, aqueous NaHCO₃ (2.4 mg/ml; pH 7.8) and centrifuged. The aqueous phase was discarded. Under the same conditions, the organic phase was washed two more times with aqueous NaHCO₃. The organic phase was washed twice with equal volumes of deionized H₂O, and dried with anhydrous Na₂SO₄. The CH₂Cl₂ was removed under a stream of nitrogen, and the sample was stored in CH₃OH at -80°C.

Isolation of epoxides

Thin-layer chromatography (TLC) of the reaction mixture was done using glass plates (20 × 20 cm) precoated with a 0.25-mm layer of silica gel 60 (EM Science, Cherry Hill, NJ). At least 60 min before chromatography, the developing chamber was lined with paper and equilibrated with mobile phase. Samples, dissolved in 10 μl of CH₂Cl₂, were applied as 1-in bands with a Teflon-tipped syringe (Scientific Glass Engineering, Austin, TX) and maintained under a nitrogen blanket until development. Plates were developed with *n*-hexane-ethyl acetate-glacial acetic acid 65:35:0.1 (v/v/v), and air-dried in a hood. Compounds were visualized either by charring or by brief exposure to iodine fumes (quantitation studies). For charring, plates were sprayed with 8% (w/v) CuSO₄ in 8% (v/v) phosphoric acid (5) and placed for 15 min in an oven maintained at 160°C.

Open-column silicic acid chromatography was used primarily to remove fatty acid products more polar than epoxides. Such products were common for incubations involving high concentrations (e.g., 3.0 eq) of *m*-CIPBA. With repeated, isocratic normal phase (NP-) HPLC, the polar side-products accumulate at the head of the column and interfere with epoxide separations. Thus, an open-

column procedure was developed to eliminate polar side-products from the epoxide fraction. In brief, ca. 30 mg of reaction mixture was suspended in 200 μ l of ethyl acetate-*n*-hexane 7.5:92.5 (v/v) and applied to a column (1.1 cm (i.d.) \times 36 cm) of silicic acid (Silicar CC-4, Mallinkrodt, Paris, KY). The silicic acid was activated earlier at 105°C for 120 min and preconditioned with 160 ml ethyl acetate-*n*-hexane 7.5:92.5 (v/v). Sample development was done at 1.3 ml/min and fractions were collected every 3.7 min (4.8 ml). Aliquots of the collected fractions were analyzed by TLC as described above. Fatty acids plus epoxides eluted by 48 ml. Products more polar than epoxides were eluted with ethyl acetate-*n*-hexane 20:80 (v/v) but were not analyzed further.

The total reaction mixture from incubations with 0.1 eq *m*-CIPBA, as well as the fatty acid-epoxide fraction recovered after open-column silicic acid chromatography, were examined using NP-HPLC. Samples were dissolved in *n*-hexane-isopropanol 100:0.175 (v/v). Aliquots (50 μ l) were injected onto a 0.46 (i.d.) \times 25 cm column (5 μ m silica particles; Ultrasphere Si, Beckman, San Ramon, CA) and developed in *n*-hexane-isopropanol 100:0.175 (v/v) at 440 psig and 1 ml/min. Components absorbing at 192 nm were collected over ice, dried under nitrogen, and suspended in CH₃OH.

Isolates of NP-HPLC were further resolved by RP-HPLC. Sample aliquots (50 μ l) were injected onto a 0.46 (i.d.) \times 25 cm column (Ultremex 5 μ m ODS particles, Phenomenex, Rancho Palos Verdes, CA) and developed in CH₃CN-H₂O 56:44 at 2000 psig and 1.5 ml/min. Components absorbing at 192 nm were collected over ice, concentrated under vacuum, and stored in CH₃OH.

For NP- and RP-HPLC analyses, absorptions at 192/237 nm and radioactivity were monitored. The outputs from two variable wavelength detectors, connected in series, were digitized (ADC #861; Nelson Analytical, Cupertino, CA) and sent to a computer (PDP-11/23; Digital Equipment Co., Maynard, MA). In addition, fractions were collected every 15 sec (NP-HPLC) or 24 sec (RP-HPLC) into glass scintillation vials. After adding 4.4 (NP-HPLC) or 5.0 (RP-HPLC) ml of scintillation fluid, samples were counted for 20 min in a scintillation counter (Tricarb, Packard Instruments, Downers Grove, IL) interfaced with the computer. By use of software developed in-house, cpm and absorption at 192 / 237 nm were plotted together (#7470A, Hewlett-Packard, Palo Alto, CA). This technique provided high sensitivity in determining and relating radioactivity and ultraviolet absorptions.

The NP- and RP-HPLC isolates, with or without derivatization, were also analyzed by capillary gas chromatography. After being dried under a nitrogen stream and suspended in isooctane, samples were injected (1 μ l) into a wall-coated (0.25 μ m dimethylpolysiloxane film; DB-1; J&W, Rancho Cordova, CA), fused-silica column

(0.25 mm (i.d.) \times 15 or 60 m). Once the column, positioned outside the chromatograph (on-column injector, J & W), had been loaded with sample, the column was plunged into the chromatograph oven (#5890, Hewlett Packard). The oven temperature was then increased in a step-like manner from 115°C to 230°C. At 230°C, the linear velocity of the carrier gas helium (99.9999% pure, Air Products) was 40 cm/sec.

To characterize the isolates and derivatives, a plot of carbon number versus log (retention time) was generated using 22:0, 23:0, 24:0, and 26:0 methyl ester standards. Individual equivalent chain length (ECL) values were determined from the interpolated log (retention times).

Identification of epoxides

Individual compounds were identified using electron impact (70 eV) mass spectrometry. The HPLC isolates, with or without prior hydrogenation, were analyzed using a quadrupole instrument (5970B, Hewlett Packard). A catalyst of 5% rhodium on aluminum was used for hydrogenations (6). In addition, hydrogenated and nonhydrogenated compounds were converted to vicinal diols as described by Chacos et al. (7). Once formed, diol products were dissolved in 50 μ l CH₃CN and 50 μ l *N*-methyl-*N*-trimethylsilyltrifluoroacetamide (Pierce Chemical Co.) and heated at 60°C for 15 min. After drying under nitrogen, the silylated compounds were suspended in isooctane and subjected to capillary gas-liquid chromatography-mass spectrometry (GLC-MS).

Quantitation of epoxide yields

Recoveries in extracts were determined radiometrically. During the quantitative studies on recoveries from incubations and extractions, silanized glassware was used.

Total epoxide recoveries were assessed radiometrically following TLC. Upon development, TLC plates were dried in a fume hood and briefly exposed to iodine fumes. The compounds were outlined, and the TLC plates were air-dried for several hours. Each fraction was scraped with a razor blade into a scintillation vial containing 1 ml H₂O, and mixed (Big Vortexer) for 10 min. Scintillation cocktail (10 ml; Universol, ICN Biomedicals, Costa Mesa, CA) was then added and mixed (Big Vortexer) for 10 min. All samples were counted (ca. 88% efficiency) for 50 min in a liquid scintillation counter (LS 350, Beckman). The external ³⁷Cs standard was used for quench monitoring.

Individual and total epoxide yields were also assessed radiometrically following NP- and RP-HPLC. In brief, compounds absorbing at 192 nm were collected into scintillation vials, and dried under a nitrogen stream. The total remaining eluent was collected into a graduated cylinder. Aliquots of the total remaining eluent were either first dried under nitrogen (20 ml, NP-HPLC) or directly used (2 ml, RP-HPLC) for radioassays. Scintillation fluid (10

ml) was added to each vial and mixed. Samples were counted for 50 min (ca. 92% efficiency) using an external standard for quench monitoring.

RESULTS AND DISCUSSION

Product analysis by TLC

Conditions cited for generating epoxides from unsaturated fatty acids vary widely with respect to incubation times and *m*-CIPBA equivalences (e.g., 8–10). In the present studies, incubations with 0.1 eq *m*-CIPBA resulted in the almost exclusive formation of A spots (mono-epoxides) (Fig. 1, lane “MIX(0.1)”). Based upon co-migrations of compounds isolated by open-column chromatography and NP-HPLC, the major A spot (R_f 0.56) consisted of Compounds I–V. The minor A spot (R_f 0.49) contained Compound VI. Similarly, the last fractions of open-column chromatography also contained Compound VI (with < 2% of Compound V). Thus, neither TLC nor open-column chromatography adequately resolved 22:6(*n*-3) reaction mixtures, even when the mixture was simplified by use of 0.1 eq *m*-CIPBA.

By mass spectrometry, Compounds IV, I, II, III, V, and VI were identified as 19,20-, 16,17-, 13,14-, 10,11-, 7,8-, and 4,5-epoxy-22:5, respectively (see below). The TLC polarity of the 22:6(*n*-3) epoxides thus increased ($\downarrow R_f$) as the number of carbons separating the oxirane ring and carbomethoxy group decreased (Fig. 1). As with epoxides from 18:1 (11), 18:3(*n*-3) (12), 20:4(*n*-6), and 20:5(*n*-3) (VanRollins, M., P. D. Frade, and O. A. Carretero, unpublished data), it may be that the closer the oxirane ring and carbomethoxy group are to each other, the greater the likelihood that both groups will simultaneously hydrogen-bond with

surface silanols. However, one anomaly occurs in the above fatty acid series—an unusually low R_f is seen for the *n*-3 epoxides. In the present study the *n*-3 epoxide 19,20-epoxy-20:5 (IV) has a lower R_f than its closest isomer 16,17-epoxy-22:5 (I). Perhaps with *n*-3 regioisomers, the oxirane ring is also close to the carbomethoxy group due to intramolecular arching (13). In summary, the TLC properties of epoxides from 22:6(*n*-3) are very similar, both in general and anomalous properties, to those observed for epoxides derived from other polyunsaturated fatty acids.

Methylated 20:5(*n*-3) was primarily converted to products more polar than (mono)epoxides when 3.0 eq *m*-CIPBA was used (Fig. 1: lane “MIX (3.0)”, B–D spots). By RP-HPLC, spots B–D contained over nine, eight, and three components, respectively. Because of limited resolution by RP-HPLC, the number of observed components per group was less than (but consistent) with the expected number of di-, tri-, and tetra-epoxy regioisomers: 15, 20, and 15, respectively. In addition, (absorption at 192 nm)/cpm ratios for the TLC groups showed the order: A > B > C > D. Since absorption at 192 nm reflects primarily double bonds (14), the observed differences in absorptivities suggested the groups differed in the number of double bonds: A > B > C > D. For the above reasons, the polar products were tentatively identified as (B) di-, (C) tri-, and (D) tetra-epoxides, respectively. Multi-epoxides derived from 18:2(*n*-6), 18:3(*n*-3), 20:4(*n*-6), and 20:5(*n*-3) (15,16, VanRollins, M., P. D. Frade and O. A. Carretero, unpublished observations) have also been observed. In the present study, traces of the 22:6(*n*-3) di-epoxides (Fig. 1, spot B) were evident by TLC when 0.3 eq but not 0.1 eq *m*-CIPBA was employed. Thus, the use of 0.1 eq *m*-CIPBA virtually eliminated the formation of unwanted side products.

Product analysis by NP-HPLC

Compared to TLC or RP-HPLC, NP-HPLC provided the best resolution with base-line separation of all products of 22:6(*n*-3) except Compounds V and VI (Fig. 2). After product identification by mass spectrometry (see below), the NP-HPLC elution order was found to be: (I), 16,17-, (II) 13,14-, (III) 10,11-, (IV) 19,20-, (V) 7,8-, and (VI) 4,5-epoxy-22:5. Thus, as with TLC and open-column chromatography, 19,20-epoxy-22:5 migrated out of sequence.

By monitoring absorption at 192 nm during NP-HPLC, not only epoxides but substrate (eluting first) could be visualized and collected. Thus, unreacted substrate could be readily isolated for further epoxide synthesis. Because reactions with 0.1 eq *m*-CIPBA resulted in virtually no polar side-products (Fig. 1, B–D spots), it was not necessary to wash the NP column between runs. Prolonged re-equilibration times, which are so characteristic of NP-HPLC, were thus avoided. However, with repeated chromatography there was a danger that autoxidation contaminants (seen best with RP-

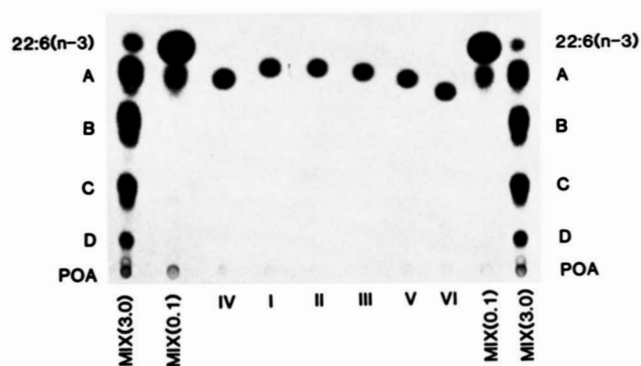


Fig. 1. Thin-layer chromatography of the epoxides derived from methylated 22:6(*n*-3). After reacting methylated 22:6(*n*-3) with either 3.0 or 0.1 eq *m*-CIPBA, reaction mixtures were applied to the outermost and next-to-outermost lanes, respectively. Spotted in more medial lanes were individual products isolated by NP-HPLC; the roman numerals refer to their NP-HPLC elution order. Upon development in *n*-hexane-ethyl acetate-glacial acetic acid 65:35:0.1 compounds were visualized by charring.

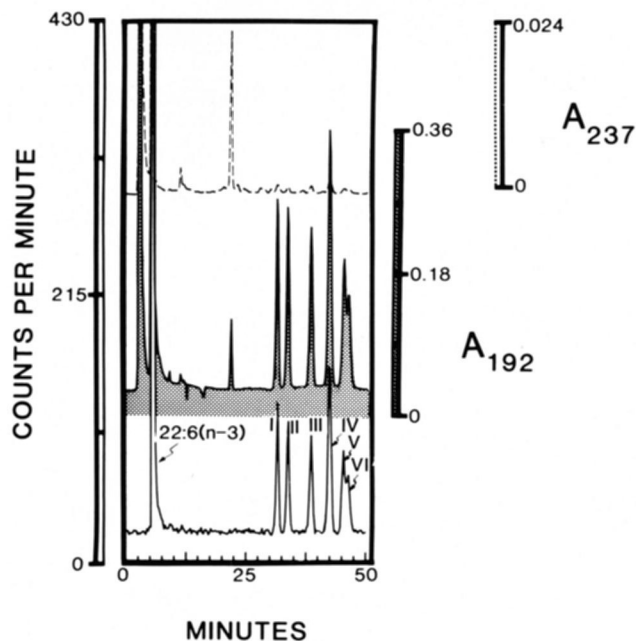


Fig. 2. Normal-phase high performance liquid chromatography of epoxides derived from methylated 22:6(n-3). After reacting methylated 22:6(n-3) with 0.1 eq *m*-CIPBA, an aliquot (21,600 dpm dissolved in 25 μ l mobile phase) was injected onto a silicic acid column. Development was with *n*-hexane-isopropanol 100:0.175 (v/v) flowing at 1.0 ml/min and at 370 psig. The column effluent, monitored at 237 nm (upper tracing) and 192 nm (middle tracing), was collected in 0.4-min fractions for radioactivity determinations (lower tracing).

HPLC) will eventually elute. For this reason, absorption at 237 nm was routinely monitored.

Product analysis by RP-HPLC

Products were resolved by RP-HPLC into five major peaks; however, only the earliest and latest eluting peaks were base-line resolved (**Fig. 3**). By adding individual NP-HPLC isolates to the product mixture, RP-HPLC peaks were found to contain IV (72 min), I (82.5 min), II + III (85.5 min), V (89.0 min), and VI (97.0 min). In particular, Compounds V and VI were widely separated by RP-HPLC. Thus, the combination of NP and RP-HPLC completely resolved all major products of 22:6(n-3) (**Table 1**).

After identification of products by mass spectrometry (see below), the RP-HPLC elution order was established to be: 19,20-, 16,17-, 13,14- plus 10,11-, 7,8-, and 4,5-epoxy-22:5. Thus, as with epoxide regioisomers of 20:4(n-6) and 20:5(n-3) (VanRollins, M., P. D. Frade, and O. A. Carretero, unpublished observations), there is a consistent pattern of elution: retention times increase as the distance between the oxirane ring and carbomethoxy groups decreases. Comparable elution patterns for the corresponding vicinal diols have been reported (reviewed in ref. 2). Such elution patterns suggest that the retention times of epoxide or diol regioisomers increase as the length of the aliphatic tail available for intercalating with ODS chains increases.

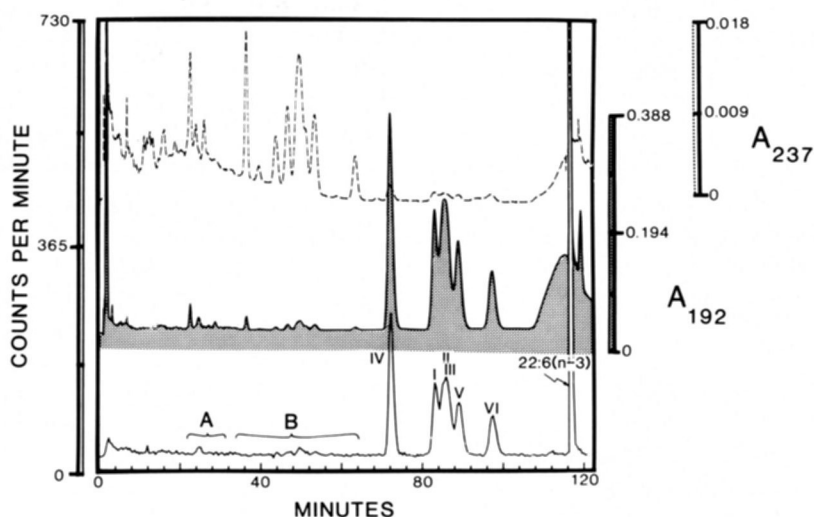


Fig. 3. Reverse-phase high performance liquid chromatography of epoxides derived from methylated 22:6(n-3). After reacting methylated 22:6(n-3) with 0.1 eq *m*-CIPBA, an aliquot of the reaction mixture (48,000 dpm dissolved in 25 μ l methanol) was injected onto an octadecasil column and resolved using acetonitrile-water 56:44 flowing at 1.5 ml/min (1780 psig). At 103 min, a linear gradient was generated over 10 min to 100% acetonitrile. The column effluent, monitored at 237 nm (upper tracing) and 192 nm (middle tracing), was collected in 0.4-min fractions for radioactivity determinations (lower tracing). Details on HPLC chromatographic conditions are provided in the Materials and Methods section.

TABLE 1. Chromatographic characterization of products from methyl docosahexaenoate

Compound	HPLC Retention Times		GLC Retention Times (Equivalent Chain Length)
	Normal Phase ^a	Reverse Phase ^b	
			<i>min</i>
I	31.3	82.5	22.7 (23.6) ^c
II	33.5	85.5	22.7 (23.5)
III	38.5	85.5	22.7 (23.5)
IV	42.4	72.0	22.7 (23.8)
V	45.6	89.0	22.7 (23.5)
VI	46.4	97.0	22.7 (23.5)

^aChromatography involved a silicic acid (5- μ m particles) column (0.46 (i.d.) \times 25 cm) developed with n-hexane-isopropanol 100:0.175 at a flow rate of 1 ml/min.

^bChromatography involved an octadecylsilyl (5- μ m ODS particles) column (0.46 (i.d.) \times 25 cm) developed with CH₃CN-H₂O 56:44 at a flow rate of 1.5 ml/min.

^cChromatography was done using a dimethylpolysiloxane film (0.25 μ m) bonded to a 0.25 mm (i.d.) \times 60 m fused-silica column. Upon injection, temperature was step-increased from 115°C to 230°C. Numbers in parentheses represent values for corresponding hydrogenated derivatives.

Other products of 0.1 eq *m*-CIPBA and 22:6(*n*-3) were also evident by RP-HPLC. Di-epoxides occurred in trace amounts (Fig. 3, 22-31 min). In addition, small amounts of autoxidation products (Fig. 3, 33-64 min) were seen. These autoxidation products were also present in un-reacted fatty acid preparations, and their levels appeared to increase with repeated exposures of substrate to air. Based on their polarities and high 237/192 absorption ratios (Fig. 3, upper and middle tracings), the autoxidation products may have been HDHE regioisomers (6), although they were not characterized further.

In summary, RP-HPLC radiochromatograms of the reaction mixtures indicated that 0.1-*eq* concentrations of *m*-CIPBA resulted primarily in the formation of epoxides from 22:6(*n*-3). Little 22:6(*n*-3) was lost due to the formation of unwanted side products.

Product analysis by capillary GLC

Products of 22:6(*n*-3) were examined by GLC using isothermal conditions and a 60-m capillary column (Table 1). Saturated fatty acid methyl ester standards, with retention times bracketing those of products, were co-injected. Each of the six 22:6(*n*-3) products had an ECL of 22.7. Thus, as with 20:4(*n*-6) and 20:5(*n*-3) epoxides (VanRollins, M., P. D. Frade, and O. A. Carretero, unpublished data), 22:6(*n*-3) epoxides were not resolved even on a 60-m column. However, resolution improved somewhat when epoxides were hydrogenated. Thereupon, Compound IV had a remarkably long retention time (ECL = 23.8, Table 1). The largest ECL in other epoxide series is generally associated with the *n*-3 epoxide (11, 16, and VanRol-

lins, M., P. D. Frade, and O. A. Carretero, unpublished data). Therefore, in agreement with the mass spectral data, Compound IV was probably 19,20-epoxy-22:5. Hydrogenated Compound I was also resolved with an ECL of 23.6. Because retention times on nonpolar phases tend to increase as the epoxy moiety is placed further and further from the carbomethoxy group, Compound I was probably 16,17-epoxy-22:5. In contrast, when the oxirane ring is located more closely to the carbomethoxy group, regioisomers are inadequately resolved, as found for epoxides derived from 18:1 (11) and 20:4(*n*-6) or 20:5(*n*-3) (VanRollins, M., P. D. Frade, and O. A. Carretero, unpublished observations). Thus, the capillary GLC data, in conjunction with other chromatographic properties (TLC, RP-HPLC and NP-HPLC) support the mass spectral identifications as (IV) 19,20-, (I) 16,17-, (II) 13,14-, (III) 10,11-, (V) 7,8-, and (VI) 4,5-epoxy-22:5.

Product analysis by mass spectrometry

Electron impact mass spectra were generated from the six products of 22:6(*n*-3) (Table 2). Spectra of underivatized products frequently possessed the following high mass ions: 358(*M*), 340(*M*-H₂O), 329(*M*-CH₃CH₂), 327(*M*-OCH₃), 315(*M*-CH₃(CH₂)₂), 311(*M*-[CH₃CH₂ + H₂O]), 297(*M*-[CH₃(CH₂)₂ + H₂O]) and 271(*M*-(CH₂)₂COOCH₃). These ions indicated an *M_r* of 358. The 358 value is 16 Da heavier than 342, the *M_r* of methyl 22:6(*n*-3), and suggested that each product possessed five double bonds and an oxirane ring. In addition, ions 329 and 311 suggested that the terminal double bond was located at C-19 and C-20.

Mass spectra were also generated after the products of 22:6(*n*-3) were catalytically hydrogenated (Table 3). High mass ions 368(*M*), 350(*M*-H₂O), 337(*M*-OCH₃), 325(*M*-CH₃(CH₂)₂), 319(*M*-[H₂O + OCH₃]), and 307(*M*-[CH₃(CH₂)₂ + H₂O]) were usually present in each spectrum, and indicated a common molecular weight of 368. Thus, hydrogenation increased the molecular mass by 10 Da (358 \rightarrow 368; Tables 2 and 3) and demonstrated that five double bonds were originally present in each of the six compounds. An *M_r* of 368 is 14 Da greater than 354, the *M_r* of methyl 22:0, and indicated the presence of an oxirane ring. In addition, ions 74, 87, 143, and 199 confirmed the basic structure of a methylated fatty acid (18). Thus, the hydrogenation studies suggested that all six compounds were oxirane derivatives of fatty acid methyl esters with five double bonds.

The mass spectrum of Compound I (Table 2) showed, inter alia, ions 289(*M*-CH₃CH₂CH=CHCH₂), 275(*M*-CH₃CH₂CH=CH(CH₂)₂), 271(*M*-[CH₃CH₂CH=CHCH₂ + H₂O]), 261 (*M*-CH₃CH₂CH=CHCH₂CO), 257 (*M*-[CH₃CH₂CH=CHCH₂ + CH₃OH]), 243(*M*-[CH₃CH₂CH=CH(CH₂)₂ + CH₃OH]), 229(*M*-[CH₃CH₂CH=CHCH₂CO + CH₃OH]), and 111(*M*-[CH₂CH=CH]₄(CH₂)₂COOCH₃). Ions 289, 271, 257,

TABLE 2. Summary of mass spectra of products derived from methyl docosahexaenoate^a

Peak I
55(52.2), 67(58.0), 69(19.9), 79(92.2), 91(100.0), 93(50.7), 105(46.1), 111(5.9), ^b 117(28.8), 119(29.1), 131(25.0), 145(13.0), 161(11.6), 166(6.2), 173(5.8), 201(1.4), 211(1.8), 213(1.7), 221(1.5), 229(0.2), ^c 239(1.7), 243(0.4), ^d 257(1.0), ^b 261(0.2), ^c 271(1.0), ^b 275(0.1), ^d 289(0.3), ^b 297(0.2), 311(0.2), 327(0.2), 329(0.2), 340(0.1), 358(0.1)
Peak II
55(45.0), 67(52.2), 79(100.0), 91(52.7), 93(45.6), 105(30.1), 117(22.7), 119(21.0), 137(3.1), 145(6.5), 151(1.6), 157(5.6), 171(4.4), 175(2.8), ^b 189(1.6), ^c 199(2.8), 203(0.6), ^d 206(3.2), 217(1.5), ^b 221(0.6), ^c 231(1.4), ^b 235(0.4), ^d 239(0.8), 249(0.3), ^b 257(0.6), 271(0.7), 297(0.2), 311(0.2), 315(0.1), 327(0.1), 329(0.1), 340(0.05), 358(0.1)
Peak III
55(46.1), 67(57.2), 79(100.0), 91(57.8), 93(46.2), 105(29.1), 117(14.4), ^b 119(23.2), 131(12.8), 147(7.6), 149(4.9), ^b 173(3.5), ^b 177(2.9), ^b 191(1.4), ^b 195(0.8), ^d 197(1.2), ^c 199(1.1), 205(0.7), ^b 209(0.4), ^b 213(1.0), 231(0.8), 239(0.5), 257(0.5), 263(0.4), 271(0.4), 297(0.1), 311(0.1), 315(0.1), 327(0.05), 329(0.05)
Peak IV
55(34.4), 57(33.8), 59(34.4), 67(68.0), 71(10.5), 77(42.9), 79(85.8), 91(100.0), 93(38.4), 105(42.5), 117(42.5), 119(30.3), 131(29.1), 145(12.3), 159(8.6), 166(4.6), 171(5.3), 185(4.2), 199(2.1), 206(2.3), 213(1.3), 232(0.7), 239(0.6), 257(0.3), 269(0.2), ^c 271(0.6), 279(0.1), ^b 286(0.1), 297(0.2), ^b 299(0.2), 301(0.1), ^c 311(0.2), ^b 327(0.1), 340(0.05)
Peak V
55(43.6), 67(68.5), 79(100.0), 91(50.5), 93(40.3), 105(23.1), 108(20.1), 117(20.1), 119(16.3), 125(8.6), ^c 131(12.4), 137(5.7), ^b 145(6.2), 157(5.8), ^c 169(1.6), ^b 173(2.7), 183(1.2), ^b 197(1.0), 199(1.0), 203(0.5), ^c 213(1.7), 217(0.4), ^d 223(0.5), 231(0.7), ^b 239(0.3), 257(0.2), 271(0.3), 285(0.1), 297(0.1), 311(0.1), 327(0.03)
Peak VI
55(48.8), 67(56.1), 79(100.0), 85(50.6), ^c 91(78.4), 93(33.6), 101(13.9), ^c 105(28.3), 111(4.7), ^b 115(14.2), ^d 117(39.0), ^c 119(22.9), 129(25.1), ^b 131(14.0), 143(6.3), 145(7.8), 157(5.6), 171(3.3), 185(2.7), 213(1.0), 215(0.7), 217(0.6), 221(0.5), 229(0.6), ^b 239(0.6), 243(0.3), ^c 253(0.3), ^b 257(0.3), ^d 271(0.3), ^b 285(0.2), ^b 297(0.2), 311(0.2), 315(0.1), 329(0.1), 340(0.1)

^aElectron impact (70 eV) mass spectra were generated from Compounds I-VI isolated from peaks labeled in Figs. 2 and 3.

^bThese ions reflect simple α - or β -cleavages to the oxirane ring (17). As with c -e, they may also reflect CH₃OH and/or H₂O losses.

^cThis ion reflects transannular cleavage with hydrogen transfer from a carbon α to the oxirane ring to yield R-CH=CH + HO=CH-R' (17).

^dThis ion reflects transannular cleavage with hydrogen transfer between carbons of the oxirane ring to generate R-C=O⁺ + CH₂-R' (11).

^eThis ion reflects cleavage similar to *d* except that the charge remains with aliphatic fragment ^eCH₂-R' (11).

and 111 reflected cleavages α to the oxirane ring. Ions 275, 261, 243, and 229 reflected transannular cleavages (for mechanisms, see Table 2 legends *c*-*e*). Together the above ions indicated an oxirane ring at C-16 and C-17. Thus, the structure of underivatized Compound I is 16, 17-epoxy-22:5.

The mass spectrum of hydrogenated Compound I (Table 3) contained ions 297(M-CH₃(CH₂)₄), 285(M-CH₃(CH₂)₃CH=CH), 283(M-CH₃(CH₂)₃), 279(M-[CH₃(CH₂)₄ + H₂O]), 269(M-CH₃(CH₂)₄CO), 265(M-[CH₃(CH₂)₄ + CH₃OH]), 253(M-[CH₃(CH₂)₃CH=CH +

CH₃OH]), 251(M-[CH₃(CH₂)₅ + CH₃OH]), 237(M-[CH₃(CH₂)₄CO + CH₃OH]), 127(M-(CH₂)₁₃COOCH₃) and 113 (M-(CH₂)₁₄COOCH₃). Thus, hydrogenation shifted the α -cleavage fragment 111 by 2 Da (Tables 2 and 3). Therefore, there was one double bond between the methyl termi-

TABLE 3. Summary of mass spectra of hydrogenated products derived from methyl docosahexaenoate^a

Peak I
55(100.0), 57(41.3), 59(14.4), 67(25.9), 69(48.2), 74(52.2), 81(24.1), 83(30.3), 87(30.5), 95(20.7), 97(24.2), 101(6.4), 109(12.0), 111(10.3), 113(15.1), ^b 127(2.8), ^b 143(10.4), 185(3.7), 199(7.2), 209(1.6), 217(1.5), 219(1.6), 225(3.7), 235(2.4), 237(2.2), ^c 251(3.5), ^d 253(1.8), ^c 265(3.8), ^b 269(6.6), ^c 279(1.1), ^b 283(0.5), ^d 285(0.3), ^c 297(10.8), ^b 307(0.3), 319(0.8), 325(0.3), 337(1.1), 350(0.1), 368(0.2)
Peak II
55(100.0), 57(50.8), 59(14.7), 69(58.6), 74(58.9), 81(29.3), 83(48.0), 87(41.3), 95(29.5), 97(27.5), 109(14.4), 111(12.6), 124(7.3), 127(7.3), 141(5.0), 143(14.5), 155(14.4), ^b 169(0.8), ^b 183(4.4), 195(3.6), ^c 199(0.7), 209(2.5), ^d 211(7.4), ^c 223(3.5), ^b 227(7.4), ^c 237(1.6), ^b 241(0.7), ^d 243(1.3), ^c 255(7.4), ^b 270(0.2), 277(0.3), 283(0.2), 293(0.3), 295(0.4), 301(0.2), 307(0.2), 319(0.7), 325(0.2), 337(0.9), 350(0.1), 368(0.2)
Peak III
55(100.0), 57(49.4), 59(15.4), 67(31.0), 69(50.0), 74(49.8), 81(28.2), 83(30.3), 87(27.6), 95(14.0), 97(15.6), 108(15.6), 111(10.6), 121(3.8), 123(6.8), 134(7.6), 141(6.1), ^b 143(1.3), 150(6.2), 153(6.2), ^c 169(25.0), ^c 179(0.4), ^b 181(1.5), ^b 185(7.0), ^c 195(0.9), 197(7.0), ^b 199(1.1), 201(1.8), ^c 209(2.5), 213(6.2), ^b 228(0.2), 237(0.2), 241(0.2), 251(0.2), 301(0.2), 319(0.4), 325(0.1), 337(0.4), 350(0.1), 368(0.1)
Peak IV
55(100.0), 57(66.8), 59(35.4), 67(31.6), 69(63.1), 71(18.1), ^b 74(65.8), 81(29.2), 83(32.8), 85(15.7), ^b 87(58.6), 95(26.8), 97(31.4), 109(14.6), 111(14.6), 123(7.8), 125(6.2), 129(4.3), 143(9.0), 199(2.6), 211(2.0), 227(2.2), 241(2.1), 261(2.0), 267(3.9), 279(3.8), ^c 289(0.8), ^b 293(4.0), ^d 307(4.5), ^b 311(2.3), ^c 319(0.6), 321(1.1), ^d 325(0.3), ^d 337(1.0), 339(7.4), ^b 350(0.1), 368(0.3)
Peak V
55(100.0), 57(60.0), 59(23.8), 67(40.5), 69(50.9), 71(25.4), 74(41.2), 79(9.8), 81(50.6), 83(50.0), 85(17.8), 87(21.8), 95(21.6), 97(25.3), 101(6.2), ^b 109(12.2), 111(29.6), ^c 115(3.1), 125(17.3), 127(93.7), ^c 143(22.2), ^c 153(2.7), ^b 157(12.6), ^d 159(12.6), ^c 167(1.5), ^b 171(9.9), ^b 185(0.7), ^b 199(0.7), 211(0.3), ^c 221(0.6), ^b 225(1.5), ^d 239(15.0), ^b 253(0.7), 267(1.3), ^b 276(0.6), 280(0.6), 294(3.0), 301(0.6), 308(0.5), 319(0.8), 325(0.2), 337(1.6), 350(0.2), 368(1.4)
Peak VI
55(80.3), 57(64.3), 59(40.6), 69(40.4), 71(34.8), 74(8.6), 83(39.7), 85(100.0), ^c 87(8.8), 97(29.5), 101(70.0), ^c 111(20.1), 115(8.7), ^d 117(64.5), ^c 125(13.8), 130(20.1), 139(2.4), 144(17.5), 157(2.9), 167(7.2), 181(1.7), 199(2.5), 227(0.2), 263(0.6), ^b 267(1.1), ^d 269(0.4), ^c 281(7.5), ^b 293(2.0), 295(1.0), ^b 301(0.7), 307(0.6), 309(0.5), 319(0.6), 325(0.5), 337(2.0), 350(0.1), 368(1.1)

^aElectron impact (70 eV) mass spectra were generated after hydrogenation of Compounds I-VI isolated from peaks labeled in Figs. 2 and 3.

^bThese ions reflect simple α - or β -cleavage to the oxirane ring (17). As with *c*-e, they may be accompanied by CH₃OH and/or H₂O losses.

^cThis ion reflects transannular cleavage with hydrogen transfer from a carbon α to the oxirane ring to yield R-CH=CH + HO⁺=CH-R' (17).

^dThis ion reflects transannular cleavage with hydrogen transfer between carbons of the oxirane ring to generate R-C=O⁺ + CH₂-R' (11).

^eThis ion reflects cleavage similar to *d* except that the charge remains with the aliphatic fragment ^eCH₂-R' (11).

nus (C-22) and the oxirane ring (C-16 and C-17). Hydrogenation also resulted in an 8 Da shift in α -cleavage fragments 289, 271, and 257, as well as in transannular-cleavage fragments 275, 261, 243, and 229 (Tables 2 and 3). Therefore, there were four double bonds between the oxirane ring and the COOCH₃ group. In summary, the mass spectral data suggested that the double-bond positions remained intact. Therefore, Compound I was identified as 16,17-(*cis*)epoxy-docosa-4,7,10,13,19-pentaenoic acid.

The electron impact mass spectrum of Compound II (Table 2) showed ions 249(M-CH₃[CH₂CH=CH]₂CH₂), 235(M-CH₃[CH₂CH=CH]₂CH₂), 231(M-[CH₃[CH₂CH=CH]₂CH₂ + H₂O]), 221(M-CH₃[CH₂CH=CH]₂-CH₂CO), 217(M-[CH₃[CH₂CH=CH]₂CH₂ + CH₃OH]), 203(M-[CH₃[CH₂CH=CH]₂(CH₂)₂ + CH₃OH]), 189(M-[CH₃[CH₂CH=CH]₂CH₂CO + CH₃OH]), and 151(M-[CH₂-CH=CH]₃(CH₂)₂COOCH₃). The ions 249, 231, 217, and 151 reflected cleavages α to the oxirane ring. The ions 235, 221, 203, and 189 reflected transannular cleavages. Each of the above ions indicated an oxirane ring at C-13 and C-14. Thus, the structure of underivatized Compound II is 13,14-epoxy-22:5.

The mass spectrum of hydrogenated Compound II (Table 3) revealed ions 255(M-CH₃(CH₂)₇), 243(M-CH₃(CH₂)₆CH=CH), 241(M-CH₃(CH₂)₈), 237(M-[CH₃(CH₂)₇ + H₂O]), 227(M-CH₃(CH₂)₇CO), 223(M-[CH₃(CH₂)₇ + CH₃OH]), 211(M-[CH₃(CH₂)₆CH=CH + CH₃OH]), 209(M-[CH₃(CH₂)₈ + CH₃OH]), 195(M-[CH₃(CH₂)₇CO + CH₃OH]), 169(M-(CH₂)₁₀COOCH₃), and 155(M-(CH₂)₁₁COOCH₃). Hydrogenation increased the α -cleavage fragment 151 by 4 Da (Tables 2 and 3). Therefore, there were two double bonds between the methyl terminus (C-22) and the oxirane ring (C-13 and C-14). Hydrogenation also shifted by 6 Da the α -cleavage fragments 249, 231, and 217, as well as the transannular-cleavage fragments 235, 221, 203, and 189 (Tables 2 and 3). Therefore, there were three double bonds between the oxirane ring and the COOCH₃ groups. The mass spectral data thus suggested that the double-bond positions remained intact. Therefore, Compound II was identified as 13,14-(*cis*)epoxy-docosa-4,7,10,16,19-pentaenoic acid.

The mass spectrum of Compound III (Table 2) contained ions 209(M-CH₃[CH₂CH=CH]₃CH₂), 205(M-[CH=CHCH₂]₂CH₂COOCH₃), 197(M-CH₃[CH₂CH=CH]₃-CH=CH), 195(M-CH₃[CH₂CH=CH]₃(CH₂)₂), 191(M-[CH₃[CH₂CH=CH]₃CH₂ + H₂O]) or (M-[CH₂CH=CH]₂(CH₂)₂COOCH₃), 177(M-[CH₃[CH₂CH=CH]₃-CH₂ + CH₃OH]), 173(M-[CH₂CH=CH]₂(CH₂)₂-COOCH₃ + H₂O]), and 149(M-CH(O)CH[CH₂CH=CH]₂(CH₂)₂COOCH₃). Ions 209, 191, 177, 173, and 149 reflected cleavages α to the oxirane ring; ion 205 reflected cleavage β to oxirane ring. In addition, ions 197 and 195 reflected transannular cleavages. Each of the above ions thus indicated an oxirane ring at C-10 and C-11. Therefore, the structure of underivatized Compound III is 10,11-epoxy-22:5.

The mass spectrum of hydrogenated Compound III (Table 3) revealed ions 213(M-CH₃(CH₂)₁₀), 201(M-CH₃(CH₂)₉CH=CH), 197(M-(CH₂)₈COOCH₃), 195(M-[CH₃(CH₂)₁₀ + H₂O]), 185(M-CH₃(CH₂)₁₀CO), 181(M-[CH₃(CH₂)₁₀ + CH₃OH]), 179(M-[(CH₂)₈COOCH₃ + H₂O]), 169(M-[CH₃(CH₂)₉CH=CH + CH₃OH]), 153(M-[CH₃(CH₂)₁₀CO + CH₃OH]), and 141(M-CH₂CH(O)CH(CH₂)₈COOCH₃). Hydrogenation apparently shifted the α -cleavage fragments 191 and 173 by 6 Da (Tables 2 and 3). Therefore, there were three double bonds between the methyl terminus (C-22) and the oxirane ring (C-10 and C-11). In addition, hydrogenation shifted by 4 Da the α -cleavage fragments 209, 191, and 177, and the transannular-cleavage fragment 197 (Tables 2 and 3). Therefore, there were two double bonds between the oxirane ring and the COOCH₃ group. The mass spectral data thus suggested that double-bond positions remained intact. Compound III was therefore identified as 10,11-(*cis*)epoxy-docosa-4,7,13,16,19-pentaenoic acid.

The mass spectrum of Compound IV (Fig. 4a) showed ions 311(M-[CH₃CH₂ + H₂O]), 301(M-CH₃CH₂CO), 297(M-[CH₃CH₂ + CH₃OH]), 279(M-[CH₃CH₂ + H₂O + CH₃OH]), and 269(M-[CH₃CH₂CO + CH₃OH]). Ions 311, 297, and 279 reflected cleavages α to the oxirane ring. Ions 301 and 269 reflected transannular cleavages. Each of the above ions indicated an oxirane ring at C-19 and C-20. Thus, the structure of underivatized Compound IV is 19,20-epoxy-22:5.

The mass spectrum of hydrogenated Compound IV (Fig. 4b) contained, inter alia, ions 339(M-CH₃CH₂), 325(M-CH₃(CH₂)₂), 321(M-[CH₃CH₂ + H₂O]), 311(M-CH₃-CH₂CO), 307(M-[CH₃CH₂ + CH₃OH]), 293(M-[CH₃(CH₂)₂ + CH₃OH]), 289(M-[CH₃CH₂ + CH₃OH + H₂O]), 279(M-[CH₃CH₂CO + CH₃OH]), 85(M-(CH₂)₁₆COOCH₃), and 71(M-(CH₂)₁₇COOCH₃). Hydrogenation apparently shifted by 10 Da the α -cleavage fragments 311, 297, and 279, and the transannular-cleavage fragments 301 and 269 (Tables 2 and 3). Therefore, five double bonds were located between the oxirane ring (C-19, C-20) and the COOCH₃ group. The mass spectral data thus suggested that the double-bond positions remained intact. Compound IV was therefore identified as 19,20-(*cis*)epoxy-docosa-4,7,10,13,16-pentaenoic acid.

The mass spectrum of Compound V (Table 2) showed ions 231(M-CH₂CH=CH(CH₂)₂COOCH₃), 217(M-(CH₂)₂CH=CH(CH₂)₂COOCH₃), 203(M-OCCH₂CH=CH(CH₂)₂COOCH₃), 183(M-CH₃[CH₂CH=CH]₄), 169(M-CH₃[CH₂CH=CH]₄CH₂), 157(M-CH₃[CH₂CH=CH]₄CH=CH), 137(M-[CH₃[CH₂CH=CH]₄CH₂ + CH₃OH]), and 125(M-[CH₃[CH₂CH=CH]₄CH=CH + CH₃OH]). Ions 231, 169, and 137 reflected cleavages α to the oxirane ring; ion 183 arose from cleavage β to the oxirane ring. Ions 217, 203, 157, and 125 reflected transannular cleavages. Each of the above ions indicated an oxirane ring at C-7 and C-8. Thus, the structure of underivatized Compound V is 7,8-epoxy-22:5.

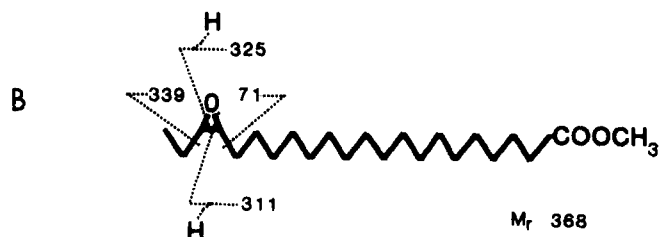
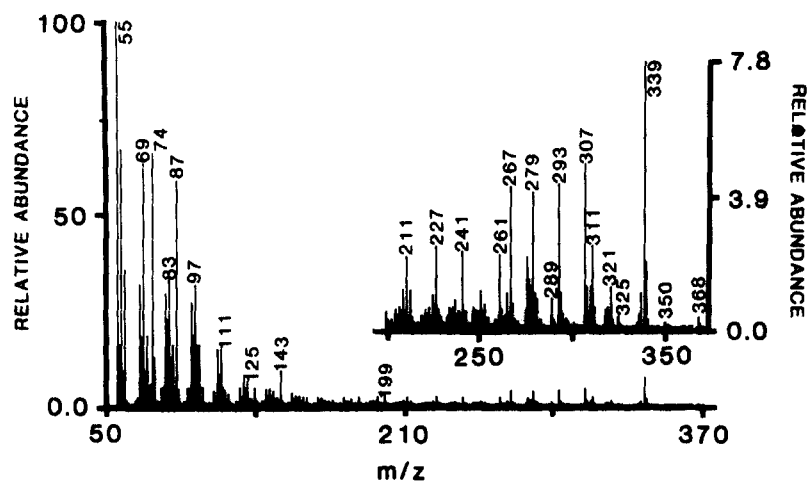
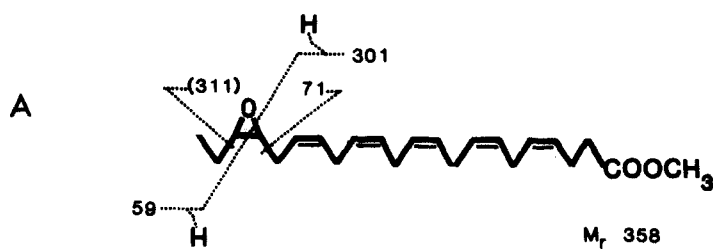
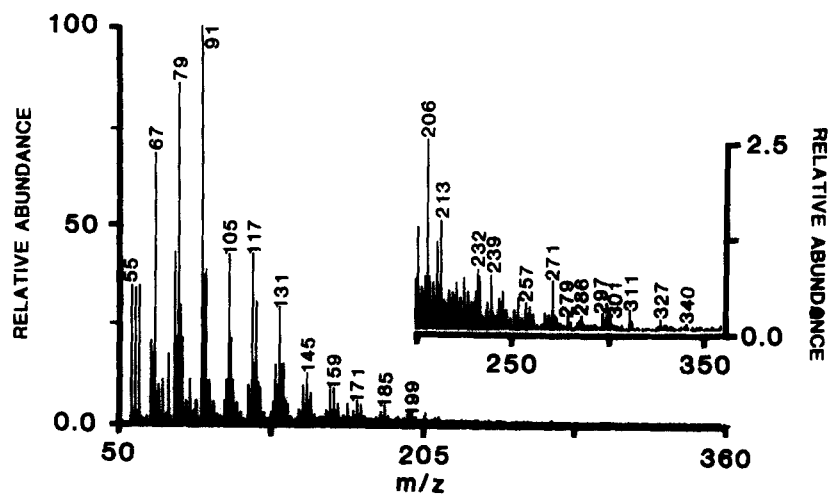


Fig. 4. Electron impact (70 eV) mass spectra of non-hydrogenated and hydrogenated Compound IV.

The mass spectrum of hydrogenated Compound V (Table 3) contained ions 294(M-H₂C=C(OH)OCH₃), 267(M-(CH₂)₃COOCH₃), 239(M-(CH₂)₅COOCH₃), 225(M-(CH₂)₆COOCH₃), 221(M-[(CH₂)₅COOCH₃ + H₂O]), 211(M-OC(CH₂)₅COOCH₃), 185(M-CH₃(CH₂)₁₂), 171(M-CH₃(CH₂)₁₃), 167(M-[CH₃(CH₂)₁₂ + H₂O]), 159(M-CH₃(CH₂)₁₂CH=CH), 157(M-CH₃(CH₂)₁₄), 153(M-[CH₃(CH₂)₁₂ + CH₃OH]), 143(M-CH₃(CH₂)₁₃CO), 127(M-[CH₃(CH₂)₁₂CH=CH + CH₃OH]), 111(M-[CH₃(CH₂)₁₃CO + CH₃OH]), and 101(M-CH₃(CH₂)₁₃-CH(O)CH(CH₂)₅COOCH₃). Hydrogenation had shifted by 8 Da the α -cleavage fragment 231 and the transannular-cleavage fragments 217 and 203. Therefore, there were four double bonds between the methyl terminus (C-22) and the oxirane ring (C-7 and C-8). In contrast, hydrogenation only shifted by 2 Da the α -cleavage fragment 169, the β -cleavage fragment 183, and the transannular-cleavage fragments 157 and 125. Thus, there was one double bond between the oxirane ring and the carbomethoxy group. The mass spectral data therefore suggested that the double-bond positions remained intact. Accordingly, Compound V was identified as 7,8-(*cis*)epoxy-docosa-4,10,13,16,19-pentaenoic acid.

The mass spectrum of Compound VI (Table 2) showed ions 285(M-CH₂COOCH₃), 271(M-(CH₂)₂COOCH₃), 257(M-(CH₂)₃COOCH₃), 253(M-[(CH₂)₂COOCH₃ + H₂O]), 243(M-OC(CH₂)₂COOCH₃), 229(M-CH(O)-CH(CH₂)₂COOCH₃), 143(M-CH₃[CH₂CH=CH]), 129(M-CH₃[CH₂CH=CH]₅CH₂), 117(M-CH₃[CH₂CH=CH]₅CH=CH), 115(M-CH₃[CH₂CH=CH]₅CH₂)₂, 111(M-[CH₃[CH₂CH=CH]₅CH₂ + H₂O]), 101(M-CH₃[CH₂CH=CH]₅CH₂CO), and 85(M-[CH₃[CH₂CH=CH]₅CH=CH + CH₃OH]). Ions 271, 253, 229, 129, and 111 reflected cleavages α to the oxirane ring; ion 285 and possibly 143 arose via β -cleavage to the oxirane ring. Ions 257, 243, 117, 115, 101, and 85 reflected transannular cleavages. Each of the above ions thus indicated an oxirane ring at C-4 and C-5. Therefore, the structure of underivatized Compound VI is 4,5-epoxy-22:5.

The mass spectrum of hydrogenated Compound VI (Table 3) contained ions 295(M-CH₂COOCH₃), 281(M-(CH₂)₂COOCH₃), 269(M-HC=CHCH₂COOCH₃), 267(M-(CH₂)₃COOCH₃), 263(M-[(CH₂)₂COOCH₃ + H₂O]), 117(M-CH₃(CH₂)₁₅CH=CH), 115(M-CH₃(CH₂)₁₇), 101(M-CH₃(CH₂)₁₆CO), and 85(M-[CH₃(CH₂)₁₅CH=CH + CH₃OH]). Thus, hydrogenation shifted by 10 Da the α -cleavage fragments 271 and 253, the β -cleavage fragment 285, and the transannular-cleavage fragment 257 (Tables 2 and 3). Therefore, five double bonds were located between the methyl terminus and the oxirane ring at C-4 and C-5. In contrast, hydrogenation did not appear to affect the transannular-cleavage fragments 117, 115, or 101. Thus, there were no double bonds between the oxirane ring and the carbomethoxy group. Accordingly, the mass spectral data suggested that the double-bond positions remained in-

tact. Therefore, Compound VI was identified as 4,5-(*cis*)epoxy-docosa-7,10,13,16,19-pentaenoic acid.

To further confirm the identities of the 20:5(*n*-3) epoxides, each product was hydrolyzed to its corresponding vicinal diol and silylated. Electron impact (70 eV) spectra of the [bis]trimethylsilyl ether, methyl ester products matched those of corresponding 22:6(*n*-3) metabolites (1). The identities of epoxides or their hydrolysis products were thus unequivocally established as IV (19,20-), I (16,17-), II (13,14-), III (10,11-), II (7,8-), and I (4,5-)epoxy- or dihydroxy-22:5, respectively.

Determination of yields

Following extractive isolation plus bicarbonate and aqueous washes, the recovered radioactivity was 99.5 \pm 0.1% (*n* = 4) of the incubated 22:6(*n*-3). Recoveries were not altered by using different *m*-CIPBA equivalences (0.3, 3.0) or by prolonging incubations to 16 hr. Thus, the extraction procedure was quantitative for both the monoepoxides and the more polar side-products.

Total and individual yields of epoxides were assessed radiometrically. The total epoxide yields, close to the theoretical 10% maximum yield (Table 4), were not increased by prolonging the incubation to 16 hr. Thus, the reaction was complete within 15 min.

The yield for an individual regioisomer decreased as the distance between its oxirane ring and carbomethoxy group decreased (Table 4). This order was also seen when higher *m*-CIPBA equivalences were used, as observed for 20:4(*n*-6) and 20:5(*n*-3) (8, 10, and unpublished data, VanRollins, M., P. D. Frade, and O. A. Carretero). This same order was also evident for the hydrolysis products of 22:6(*n*-3) epoxides formed by microsomes fortified with NADPH (1).

TABLE 4. Epoxide yield from methyl docosahexaenoate

Compound	Radioactivity ^a
	%
22:6(<i>n</i> -3)	89.2 \pm 0.3 (88.6 \pm 0.2)
Monoepoxides	
19,20-	2.5 \pm 0.1
16,17-	1.5 \pm 0.1
13,14-	1.3 \pm 0.1
10,11-	1.2 \pm 0.1
7,8-	1.2 \pm 0.1
4,5-	0.9 \pm 0.03
Total	8.6 \pm 0.4 (9.3 \pm 0.1)
Diepoxides ^b	0.3 \pm 0.03

^aData represent means \pm SD (*n* = 4) of total radioactivity recovered after RP-HPLC. Corresponding TLC values are in parentheses. The total collected radioactivity represented 102.4 \pm 3.3% (RP-HPLC) and 95.6 \pm 3.0% (TLC) of the applied radioactivity.

^bOther minor components were probably autoxidation artifacts (HDHEs, see ref. 6) and represented 0.4 \pm 0.1% of the total radioactivity.

Minor products were also evident in the reaction mixtures (Table 4). Trace amounts (0.3%) of products more polar than mono-epoxides (Fig. 3, A group) were detected. In addition, trace amounts (0.4%) of autoxidation products were also evident (Fig. 3, B group). This level of autoxidation products was also seen with the nonincubated 22:6(n-3). Apparently, the trace levels of autoxidation products appeared when 22:6(n-3) was stored under argon in methanol at -80°C for several months. Significantly, the use of 15-min incubations did not increase the formation of autoxidation products.

Comparisons of TLC and HPLC values indicate excellent agreement between the two techniques (Table 4). However, two problems were evident with the TLC procedure. First, the total recovery of radioactivity was slightly lower with TLC than with HPLC. The lower recoveries may have been due to adsorption losses or to lack of 2 π counting conditions caused by the silica gel deposit at the bottom of the scintillation vial. Second, total epoxide values were higher with TLC than with HPLC. Part of this discrepancy may be due to the measured 1-2% trailing of 22:6(n-3) which occurs in the mono-epoxide region on the TLC plate.

In the case where large amounts of 22:6(n-3) are being used as substrate, epoxide yields are limited only by column capacities. Compounds 7,8-epoxy-22:5 (V) and 4,5-epoxy-22:5 (VI), partially overlapping during NP-HPLC (Fig. 2), are widely separated during RP-HPLC (Fig. 3). Therefore, it is the capacity of the NP-HPLC column, not the RP-HPLC column, which limits epoxide yields. Specifically, preservation of base-line separations between 16,17-epoxy-22:5 (I) and 13,14-epoxy-22:5 (II) limited the overall yields (Fig. 2). Under these circumstances, only 300 μg of reaction mixture could be safely applied. Thus, the capacity of an analytical column (0.46 cm i.d.) for the summed epoxides was 25.8 μg (8.6% (Table 4) of 300 μg). Accordingly, individual capacities were only 7.5 (2.5% of 300 μg), 4.5, 3.9, 3.6, 3.6, and 2.7 μg for 19,20-, 16,17-, 13,14-, 10,11-, 7,8-, and 4,5-epoxy-22:5, respectively. Such a limited column capacity is expected to increase 10- to 20-fold when "heart-cutting" techniques and semi-preparative columns (1.0 cm i.d.) are used (19).

In the case where small amounts of 22:6(n-3) are being used as substrate, epoxide yield is limited by the amount of side-products formed. Under these circumstances, use of 0.1 eq. *m*-CIPBA and recycling of unused substrate have definite advantages. Given an 8.6% yield per cycle, a total yield of about 55% and 70% is expected to be achieved within 10 or 20 cycles, respectively. This 55-70% yield is significantly higher than the 36% yield reported for deuterated 20:4(n-6) when 1.05 eq of *m*-CIPBA was used (8). In that study, most of the deuterated 20:4(n-6) was converted to (unidentified) polar side-products.

In conclusion, use of 0.1 eq *m*-CIPBA resulted in close to the maximum theoretical yield with minimal losses of 22:6(n-3) to side-products. The unused 22:6(n-3) was quantitatively recovered for further epoxide synthesis. Thus, by cycling techniques, labeled 22:6(n-3) may be efficiently converted to labeled epoxides. Such epoxide tracers, when made from $[1-^{14}\text{C}]22:6(n-3)$, may be used to study epoxide stability in blood, or epoxide uptake and metabolism by peripheral tissues (3). Likewise, epoxide tracers, when prepared from $[1-^{18}\text{O}_2]22:6(n-3)$ (20), may be used as internal standards for mass spectrometry to measure in vivo concentrations of docosenoids (3). Use of these epoxide tracers may help determine whether tissue concentrations of cytochrome P-450 metabolites increase following the ingestion of fish oils. ■■

This work was supported in part by NIH Research Grant number HL-28982-05 of the National Heart, Lung, and Blood Institute, and by the American Heart Association. We wish to acknowledge the expert technical assistance of Mr. J. Richard Cook. We thank Mr. Carl Polomski (Hypertension Research Division) for developing the software to acquire and plot three chromatograms. We also thank Dr. Norman Radin (University of Michigan, Ann Arbor, MI) for assistance in the TLC of epoxides. Lastly, we are deeply grateful to Dr. J. R. Falck (University of Texas Health Science Center, Dallas, TX) for his helpful suggestions on the preparation of epoxide standards.

Manuscript received 19 April 1988 and in revised form 22 July 1988.

REFERENCES

1. VanRollins, M., R. C. Baker, H. W. Sprecher, and R. C. Murphy. 1984. Oxidation of docosahexaenoic acid by rat liver microsomes fortified with NADPH. *J. Biol. Chem.* **259**: 5776-5783.
2. VanRollins, M., P. D. Frade, and O. A. Carretero. 1988. Oxidation of 5,8,11,14,17-eicosapentaenoate by hepatic and renal microsomes. *Biochim. Biophys. Acta* **966**: 133-149.
3. Falck, J. R., V. J. Schueler, H. R. Jacobson, A. K. Siddhanta, B. Pramanik, and J. Capdevila. 1987. Arachidonate epoxidase: identification of epoxyeicosatrienoic acids in rabbit kidney. *J. Lipid Res.* **28**: 840-846.
4. Chung, S. K., and A. I. Scott. 1974. Synthesis of (\pm)-eicosacis-8,9-(11,12- and 14,15)-epoxy-cis-11,14-(8,14- and 8,11)-dienoic acids and attempted bioconversion to prostaglandins. *Tetrahedron Lett.* **35**: 3023-3024.
5. Touchstone, J. C., S. S. Levin, M. F. Dobbins, and P. J. Carter. 1981. Differentiation of saturated and unsaturated phospholipids on thin-layer chromatograms. *J. High Resol. Chromatogr. Chromatogr. Commun.* **2**: 423-424.
6. VanRollins, M., and R. C. Murphy. 1984. Autooxidation of docosahexaenoic acid: analysis of ten isomers of hydroxydocosahexaenoate. *J. Lipid Res.* **25**: 507-517.
7. Chacos, N., J. R. Falck, C. Wixtrom, and J. Capdevila. 1982. Novel epoxides formed during the liver cytochrome P-450 oxidation of arachidonic acid. *Biochem. Biophys. Res. Commun.* **104**: 916-922.

8. Oliw, E. H., and P. Moldeus. 1982. Metabolism of arachidonic acid by isolated rat hepatocytes, renal cells and by some rabbit tissues. *Biochim. Biophys. Acta.* **721**: 135-143.
9. Fitzpatrick, F. A., M. D. Ennis, M. E. Baze, M. A. Wynalda, J. E. McGee, and W. F. Liggett. 1986. Inhibition of cyclooxygenase activity and platelet aggregation by epoxy-eicosatrienoic acids: influence of stereochemistry. *J. Biol. Chem.* **261**: 15334-15338.
10. Oliw, E. H., F. P. Guengerich, and J. A. Oates. 1982. Epoxidation of arachidonic acid by hepatic monooxygenases: isolation and metabolism of four epoxide intermediates. *J. Biol. Chem.* **257**: 3771-3781.
11. Gunstone, F. D., and F. R. Jacobsberg. 1972. Fatty acids, part 35. The preparation and properties of the complete series of methyl epoxyoctadecanoates. *Chem. Phys. Lipids.* **9**: 26-34.
12. Oliw, E. H. 1983. Analysis of 1,2-diols of linoleic, α -linolenic and arachidonic acid by gas chromatography-mass spectrometry using cyclic alkyl boronic esters. *J. Chromatogr.* **275**: 245-259.
13. Corey, E. J., S. Iguchi, J. O. Albright, and B. De. 1983. Studies on the conformational mobility of arachidonic acid. Facile macrolactonization of 20-hydroxyarachidonate. *Tetrahedron Lett.* **24**: 37-40.
14. Avelaño, M. I., M. VanRollins, and L. A. Horrocks. 1983. Separation and quantitation of free fatty acids and fatty acid methyl esters by reverse phase high pressure liquid chromatography. *J. Lipid Res.* **24**: 83-93.
15. Vacheron, M. J., G. Michel, and R. Guilluy. 1969. Localisation des doubles liaisons dans les acides ethyleniques par spectrometrie de masse. *Bull. Soc. Chim. Biol.* **51**: 177-185.
16. Emken, E. A. 1972. *Cis* and *trans* analysis of fatty esters by gas chromatography: octadecanoate and octadecadienoate isomers. *Lipids.* **7**: 459-466.
17. Aplin, R. T., and L. Coles. 1967. A simple procedure for localization of ethylenic double bonds by mass spectrometry. *Chem. Commun.* 858-859.
18. McCloskey, J. A. 1969. Mass spectrometry of lipids and steroids. *Methods Enzymol.* **14**: 382-450.
19. Snyder, L. R., and J. J. Kirkland. 1979. Introduction to Modern Liquid Chromatography. 2nd ed. John Wiley and Sons, Inc., New York. 615-661.
20. Murphy, R. C., and K. L. Clay. 1982. Preparation of ^{18}O derivatives of eicosanoids for GC-MS quantitative analysis. *Methods Enzymol.* **86**: 547-551.